Impact of Annealing on T_C and Structure of Titanium Thin Films

Beatrice Siri, Edvige Celasco, Lorenzo Ferrari Barusso, Francesco Buatier de Mongeot, Pietro Manfrinetti, Giacomo Manzato, Alessia Provino, and Flavio Gatti

***Abstract*—Transition-edge sensors (TES) are superconducting devices used for detecting particles and electromagnetic radiation, ranging from γ-ray to mm wavelengths. A fundamental parameter for operations of TES detectors for the desired application is the superconducting critical temperature T_C. We are developing TES based bolometers made of metallic Ti films, with an operating temperature of 500 mK, to be used for cosmic microwave background (CMB) measurements. We have observed that electron-beam evaporation grown Ti films can reach critical temperatures higher than 500 mK when the substrate temperature is kept below some temperature threshold. Discordant critical temperatures of Titanium TES are found in literature and very little information is available about the various T_C and relative fabrication process. Critical temperature of Ti films is generally known to be affected by deposition methods, substrates, processing conditions and heating. In the past we tried to tune the critical temperature of titanium thin films by means of post-annealing and we found a regular decrease of T_C from 540 mK to 360 mK, in this work we confirm this effect. Further, we have found that titanium film grows with a most stable *hcp* structure. The annealing process until 260 °C, does not modify the morphological features of the film. We find also evidences of a shift in XRD peaks that indicate structural changes of the lattice parameters, which could play a role in the T_C modification.**

***Index Terms*—Critical temperature, morphological and structural analysis, Superconducting transitions, TES, Thin Film.**

I. Introduction

It HAS been received the assignment to develop TES bolometers for the balloon-borne millimeter-wave telescope SWIPE of the LSPE mission. The LSPE experiment is aimed at searching the B-mode polarization in the CMB. By exploiting the whole CMB polarization signal at low multipole number $l \lesssim 10$, it is possible to estimate the B-modes content down to 10^{-2} of the *r*-parameter, i.e., the so-called tensor-to-scalar ratio [1]–[3]. These large-area and multi-mode bolometers will be placed onto the focal plane of the SWIPE telescope, that is cooled to about 300 mK by a He-3 fridge. Using EM multi-mode horns to collect large microwave power, they can achieve better signal-to-noise ratio than single mode bolometers, but they need to work at higher temperatures. In fact, considering that the average optical power is about 10 pW and the thermal conductance G must be ≥ 50 pW/K, to meet the bolometer time constant requirement τ 10 ms, it is necessary a $T_C \simeq 500$ mK [4], [5]. It has been reported that titanium TES have T_C as high as 0.6 K, but it is strongly dependent on fabrication processes and substrates [6]–[9]. For instance, in Posada *et al.* [10] it is stated that the T_C of Ti/Au bilayer films is affected by deposition base pressure and processing conditions after patterning, and it has also observed that heating the samples may result in a decrease of T_C. In a previous work [11] we have observed that post-annealing of the Ti film grown in e-beam regularly reduces T_C when increasing the annealing temperature. We have concentrated our investigations on pure Ti films, to establish the causes.

Manuscript received December 1, 2020; revised February 25, 2021; accepted March 18, 2021. Date of publication April 8, 2021; date of current version June 11, 2021. This work was supported by INFN within the LSPE project and ASI within the COSMOS project. *(Corresponding author: Beatrice Siri.)*

Beatrice Siri, Edvige Celasco, Lorenzo Ferrari Barusso, and Flavio Gatti are with the Dipartimento di Fisica, Università degli Studi di Genova, 16146 Genova, Italy, and also with the INFN sezione di Genova, 16146 Genova, Italy (e-mail: beatrice.siri@ge.infn.it).

Francesco Buatier de Mongeot and Giacomo Manzato are with the Dipartimento di Fisica, Università degli Studi di Genova, 16146 Genova, Italy.

Pietro Manfrinetti and Alessia Provino are with the Dipartimento di Chimica, Università degli Studi di Genova, 16146 Genova, Italy.

Color versions of one or more figures in this article are available at https://doi.org/10.1109/TASC.2021.3071997.

Digital Object Identifier 10.1109/TASC.2021.3071997

II. Experimental Details

A. Thin Films Preparation

Titanium thin films are grown with e-beam evaporation onto a low stress low pressure chemical vapor deposition (LPCVD) Si_3N_4 substrate, 1.5 μm thick, that is deposited onto a silicon wafer (100 oriented) coated with a 0.3 μm SiO_2 thermal layer. The film's samples are grown onto 5 mm $\times$ 5 mm chips, diced from a wafer. The e-beam evaporation is performed at a background vacuum lower than 3×10^{-8} mbar. Usually, the substrate temperature is not monitored during the deposition process, but it is extrapolated from its final temperature that it stays below 80 °C for the whole process. All sample discussed in this paper are grown together in a single deposition process. The growth process is controlled by a thickness monitor that is settled at a nominal rate of 7.0 Å/s and a total thickness of 100.0 nm. The final measured values of deposition rate and final thickness are 7.2 Å/s, within 4 % uncertainty, and 86 nm, within 4 % uncertainty, respectively. Afterwards, the samples are stored in a vacuum cabinet, even if they are exposed to atmosphere for many hours, when handled for making electric contacts and for mounting on the dilution fridge, therefore, a titanium oxide passivation surface layer is expected.

This work is licensed under a Creative Commons Attribution 4.0 License. For more information, see https://creativecommons.org/licenses/by/4.0/

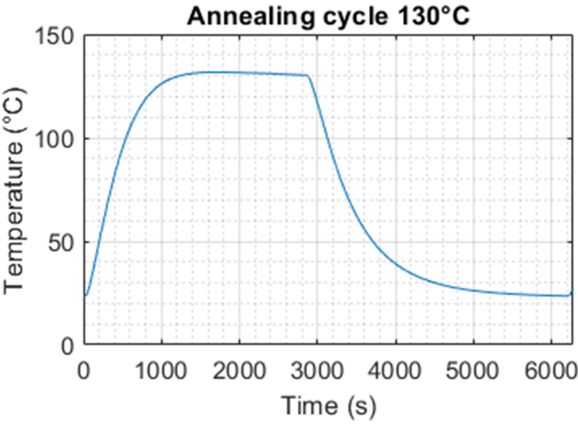

Fig. 1. An example of temperature profile of the annealing process of Ti films at 130 °C in argon atmosphere.

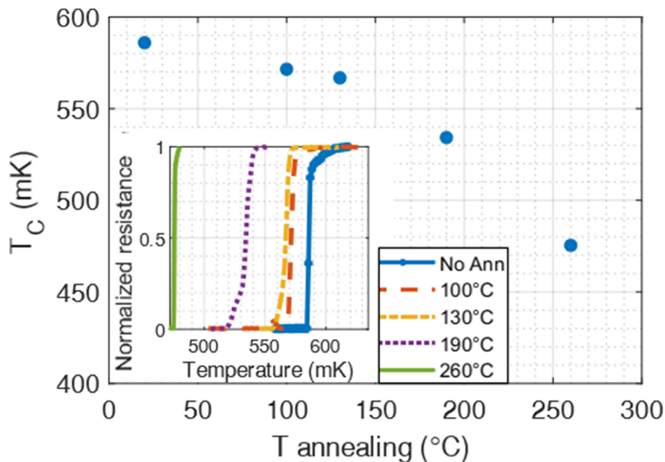

Fig. 2. Critical temperatures T_C of Ti films on Si_3N_4 substrate vs annealing temperatures. In the inset: the normalized resistance *R/Rn* curves at the super conducting to normal transition of the films.

B. Annealing Process

The annealing process is performed in Argon atmosphere to avoid further oxidation of films. Each sample is placed in an 80 mm diameter cylindrical quartz chamber which is flushed with Argon at 9 l/min to dilute possible contamination from the chamber itself. The chamber is partially at room temperature and partially in the oven, settled at the wanted temperature. The samples are mounted on a copper holder and inserted in the room temperature side of the chamber for the degassing phase. The annealing phase starts when the sample is moved to the hot part of the chamber. The film temperature during the annealing is monitored continuously with a platinum thermistor in close thermal contact with the copper sample holder. In Fig. 1 a typical annealing process is shown: the 10%-90% heating time is about 10 min, the annealing time is 30 min, the 90%-10% cooling time is 20 min. The sample is removed from the oven when it reaches room temperature. Here we consider 5 film's samples: not annealed, and annealed at the nominal temperatures of 90 °C, 130 °C, 190 °C and 260 °C respectively. For each annealing temperature two 5 mm $\times$ 5 mm Ti coated wafer pieces are processed together: one of them is used for T_C measurements, the other one for morphological characterization. The reference samples for the not annealed films are also from the same evaporation.

C. Critical Temperature

The resistances of films are measured with the four-point probe method on the cold finger of a dilution fridge. The measurements are carried out with a resistance bridge during the computer-controlled step heating of the cold sample holder. The measurement's power is less than 10 pW. Critical temperatures are estimated at the central values of the superconducting to normal-conducting transition curves. These are plotted vs the annealing temperatures in Fig. 2. The T_C of Ti films decreases as the annealing temperature increases. The sample annealed at the temperature of 260 °C, for example, shows a T_C reduction of about 18%. In the following sections we show the ongoing analysis to unveil the causes of this effect.

TABLE I
GRAIN SIZE ANALYSIS

Sample	Grain size by XRD (nm)	Grain size by AFM (nm)
Not Annealed	164	191
Tann 100 °C	167	
Tann 130 °C	155	
Tann 260 °C	151	194

Average grain size of Ti films calculated by XRD Debye-Scherrer equation, are reported in the second column and values obtained by AFM in the third one.

D. Morphological Characterization

The first evidence obtained from the morphological characterizations of Titanium film is about uniformity of the grain size in the microstructure. It is worth to note that in literature the correlations between grain size and annealing temperature have already been reported. Even if in different systems, *Matthews et al.* reported an enhancement in grain size of TiO_2 nanoparticles versus an increase of the annealing temperature ranging from 400 to 600 °C [12]. Despite the nature of this latter system and the growing method were different (dip coating), we wanted to check if this effect could be present also in the case of Titanium film deposited by e-beam. Therefore, we investigate if possible variations of the grain size could be dependent on the annealing temperature; to this aim, we use both X-ray diffraction (XRD, Panalytical PW1830; Co-Kα radiation) and Atomic Force Microscopy (CSI Nano-Observer AFM) methods. To estimate the grain size by XRD the Debye-Scherrer equation (1) is employed:

$$D = 0.9\frac{\lambda}{\cos\theta \cdot W} \tag{1}$$

where: D is the average grain size, $\lambda = 0.178901$ nm is the wavelength of Co-Kα source, θ is the diffraction peak angle and W the FWHM of peak. The main grain dimension obtained by XRD and AFM are reported in Table I.

In the relatively narrow range of temperature of the present experiment (no annealing to 260 °C), XRD does not suggest a

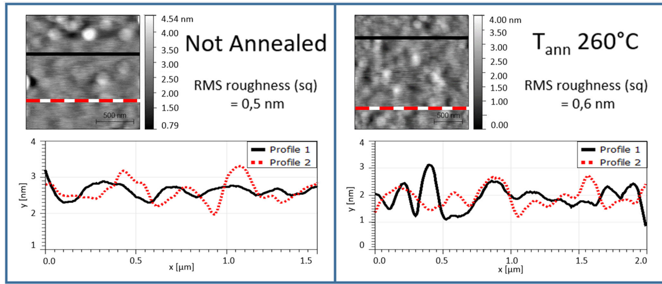

Fig. 3. AFM images in top panels: not annealed film (left) and 260 °C film (right); example of two profiles for each image are in the bottom of each panel.

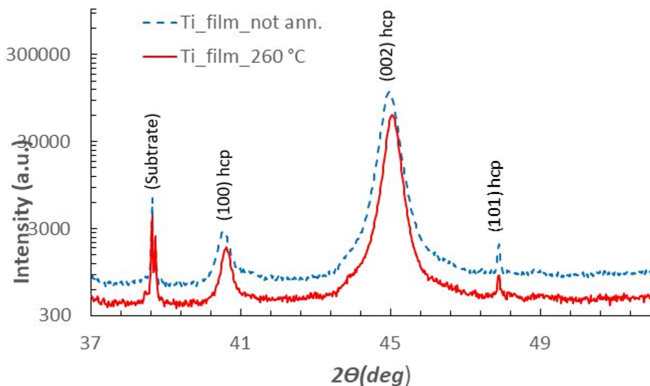

Fig. 4. XRD spectra of not annealed sample (dotted blue line) and 260 °C annealed one (continuous red line).

linear trend of grain sizes with increasing annealing temperature; this result, however, needs further confirmation. Anyway, the estimated values show a relative stability in the grain dimension that agrees with those obtained from direct measurements with AFM. The values obtained by AFM for the lower and the higher annealing temperatures are reported in Table I. In Fig. 3 the AFM scans of both samples are reported.

The AFM investigation shows a good quality of the film, and no considerable variation in the mean grain size of the 260 °C annealed sample temperature respect to the not annealed one. These aspects are confirmed also with the scanning electron microscopy images (not shown). The not annealed sample has a mean grain size of 191 nm, with values spanning from 174.7 nm to 206.7 nm, while the 260 °C annealed sample has 194 nm, with values from 171.9 nm to 214.7 nm. The calculated RMS roughness is 0.5 nm for the not annealed sample (Fig. 3 left panel), and 0.6 nm for the 260 °C annealed one (Fig. 3 right panel). RMS roughness here presented are calculated considering all the investigated area.

This is clear evidence that no noticeable morphological changes occur during the annealing.

E. Structural Analysis

Another possible cause of the *Tc* lowering after the annealing procedure could be investigated in the crystalline structures of the samples. It has been observed that Ti films exhibit hexagonal *hcp* and the uncommon cubic *fcc* structures, depending on growth conditions [13]–[15]. The former is the most stable lattice configuration.

In Fig. 4 are reported the XRD spectra of the not annealed (dotted blue line) and the annealed at 260 °C (continuous red line) samples, both acquired with a Co-Kα source.

The main line (002), at 45.0 degrees, is a clear indication of *hcp* grain orientation, combined with the presence of *hcp* satellite features (100) and (101), at 40.6 degrees and 47.9 degrees respectively. The peak at 38.7 degrees is, on the contrary, assigned to the Si-Si_3N_4 substrate.

In particular it has been reported by Arshi, et *al.* that e-beam evaporation favours the growth along the instable cubic *fcc* structure [16]. In our samples we do not have any evidence of a signal related to this *fcc* structure. The lack of this configuration in favour of the more stable *hcp* is probably linked to different evaporation conditions. Although the type of evaporation methods is the same, we operate with different parameters: lower base pressure and lower substrate temperature, as stated in Section II-A.

It seems that it is not possible to obtain the less stable *fcc* configuration using post-deposition annealing, at least in the range of temperatures considered in this article (up to 260 °C), since the samples are mainly composed of hexagonal structure.

The presence of the most stable *hcp* configuration in both samples excludes possible effect on the variation of the T_C after annealing, at least in our observed range.

Another aspect is the small shift, less than 1 deg, of the (*002*) line of the annealed sample at 260 °C compared to the not annealed one (See Fig. 4). This behaviour may originate from the relaxation of structural stresses of the lattice by the annealing and could have an influence for the final T_C observed variation, as reported.

The last hypothesis, under investigation, is that native oxygen could perform an interdiffusion in the film, during the annealing process, modifying the resistivity of the film and consequently the final T_C [17].

III. Conclusion

The decrease of T_C of Ti films with increasing annealing temperatures is reproducible and confirms the past preliminary experiments [11]. The structural and morphological parameters seem to have no effect on T_C. The indication of the observed small changes of lattice parameter could be the cause. Quantitative formulations of the effect need further detailed analysis. We cannot exclude others possible effects, as oxygen diffusion in the bulk, but we believe that we can rule out other trivial causes, like contaminations.

Acknowledgment

The authors would like to thank Luigi Parodi and Sergio Burioli for providing the low temperature set-up.

REFERENCES

[1] L. Lamagna *et al.*, "Progress report on the large-scale polarization explorer," *J. Low. Temp. Phys.*, vol. 200, no. 5-6, pp. 374–383, Sep. 2020.

[2] F. Columbro *et al.*., "SWIPE multi-mode pixel assembly design and beam pattern," *J. Low. Temp. Phys.*, vol. 199, no. 1-2, pp. 65–72, Apr. 2020.

[3] M. Biasotti *et al.*., "Fabrication and test of large area spider-web bolometers for CMB measurements," *J. Low. Temp. Phys.*, vol. 184, no. 3-4, pp. 652–646, Aug. 2016.

[4] G. P. Pepe, R. Cristiano, and F. Gatti, "Superconducting radiation and particle detectors: Superconducting hot electron bolometers and transition edge sensors," *Appl. Supercond., Handbook Devices Appl.*, vol. 2-2, pp. 860–880, Jan. 2015.

[5] R. Gualtieri *et al.*., "Multi-mode TES bolometer optimization for the LSPE-SWIPE instrument," *J. Low. Temp. Phys.*, vol. 184, no. 3-4, pp. 527–533, Aug. 2016.

[6] R. O'Brient *et al.*, "Antenna-coupled TES bolometers for the keck array, spider, and Polar-1," in *Proc. SPIE 8452, Millimeter, Submillimeter, Far-Infrared Detectors Instrum. Astron. VI*, Sep. 2012, Art. no. 84521G, doi: 10.1117/12.927214.

[7] J. A. Bonetti *et al.*, "Characterization of antenna-coupled TES bolometers for the spider experiment," *IEEE Trans. Appl. Supercond.*, vol. 19, no. 3, pp. 520–523, Jun. 2009.

[8] Z. Wang *et al.*, "Electron-beam evaporated superconducting titanium thin films for antenna-coupled transition edge sensors," *IEEE Trans. Appl. Supercond.*, vol. 28, no. 4, Jun. 2018, Art no. 2100204.

[9] D. Fukuda *et al.*, "Titanium-based transition-edge photon number resolving detector with 98% detection efficiency with index-matched small-gap fiber coupling," *Opt. Exp.*, vol. 19, no. 2, pp. 870–875, Jan. 2011.

[10] C. M. Posada *et al.*, "Fabrication of large dual-polarized multichroic TES bolometer arrays for CMB measurements with the SPT-3G camera," *Supercond. Sci. Technol.*, vol. 28, Aug. 2015, Art. no. 094002.

[11] D. Vaccaro *et al.*., "Tuning the TC of titanium thin films for transition-edge sensors by annealing in argon," *J. Low. Temp. Phys.*, vol. 193, pp. 1122–1128, Oct 2018.

[12] N. R. Matthews *et al.*, "TiO2 thin films – influence of annealing temperature on structural, optical and photocatalytic properties," *Sol. energy*, vol. 83, no. 9, pp. 1499–1508, Sep 2009.

[13] P. Scardi *et al.,* "Residual strain in deuterated ti thin films," *Mater. Lett.,* vol. 36, pp. 1–6, 1998.

[14] Y.-K. Song *et al.*., "The structural and mechanical properties of ti films fabricated by using RF magnetron sputtering," *J. Korean Phys. Soc.*, vol. 51, no. 3, pp. 1152–1155, Sep. 2007.

[15] S. K. Kim *et al.,* "Growth of face-centred-cubic titanium on aluminium," *J. Phys.: Condens. Matter*, vol. 8, pp. 25–36, 1996.

[16] N. Arshi *et al.*., "Thickness effect on properties of titanium film deposited by d.c. magnetron sputtering and electron beam evaporation techniques," *Bull. Mater. Sci.,* vol. 36, no. 5, pp. 807–812, Oct. 2013.

[17] A. P. Broumas, N. M. Degnan, and M. L. Meier, "Diffusion of oxygen in titanium," in *Proc. Amer. Soc. Eng. Educ. Annu. Conf. Expo,* 2003, doi:10.18260/1-2--11928